NIH Public Access
Author Manuscript
Cancer Discov. Author manuscript; available in PMC 2014 June 01.

Published in final edited form as:
Cancer Discov. 2013 December ; 3(12): . doi:10.1158/2159-8290.CD-13-0183.

A drug repositioning approach identifies tricyclic antidepressants as inhibitors of small cell lung cancer and other neuroendocrine tumors

Nadine S Jahchan[1,2], **Joel T Dudley**[1,§], **Pawel K Mazur**[1,2,§], **Natasha Flores**[1,2], **Dian Yang**[1,2], **Alec Palmerton**[1,2], **Anne-Flore Zmoos**[1,2], **Dedeepya Vaka**[1,2], **Kim QT Tran**[1,2], **Margaret Zhou**[1,2], **Karolina Krasinska**[3], **Jonathan W Riess**[4], **Joel W Neal**[5], **Purvesh Khatri**[1,2], **Kwon S Park**[1,2], **Atul J Butte**[1,2,*], and **Julien Sage**[1,2,*]

[1]Department of Pediatrics, Stanford University, CA 94305, USA

[2]Department of Genetics, Stanford University, CA 94305, USA

[3]Vincent Coates Mass Spectrometry Laboratory, Stanford University, CA 94305, USA

[4]University of California Davis Cancer Center, Division of Hematology/Oncology, Department of Internal Medicine, University of California Davis School of Medicine, Sacramento, CA 95817, USA

[5]Department of Medicine-Oncology, Stanford University, CA 94305, USA

Abstract

Small cell lung cancer (SCLC) is an aggressive neuroendocrine subtype of lung cancer with high mortality. We used a systematic drug-repositioning bioinformatics approach querying a large compendium of gene expression profiles to identify candidate FDA-approved drugs to treat SCLC. We found that tricyclic antidepressants and related molecules potently induce apoptosis in both chemonaïve and chemoresistant SCLC cells in culture, in mouse and human SCLC tumors transplanted into immunocompromised mice, and in endogenous tumors from a mouse model for human SCLC. The candidate drugs activate stress pathways and induce cell death in SCLC cells, at least in part by disrupting autocrine survival signals involving neurotransmitters and their G protein-coupled receptors. The candidate drugs inhibit the growth of other neuroendocrine tumors, including pancreatic neuroendocrine tumors and Merkel cell carcinoma. These experiments identify novel targeted strategies that can be rapidly evaluated in patients with neuroendocrine tumors through the repurposing of approved drugs.

[*]To whom correspondence should be addressed: Julien Sage, 265 Campus Drive, SIM1 G2078, Stanford CA 94305-5457. julsage@stanford.edu. Phone: 1-650-724-9246. Fax: 1-650-736-0195. Atul Butte, 251 Campus Drive, MSOB X163, Stanford CA 94305-5415. abutte@stanford.edu. Phone: 1-650-725-1337. Fax: 1-650-723-7070.
[§]equal contribution.

Disclosure of Potential Conflicts of Interests: Patents have been filed and are pending on the use of specific tricyclic antidepressants in neuroendocrine tumors. A.B., J.D., J.S., and N.J. are inventors on the patent, and could benefit with royalties. The intellectual property has been licensed to NuMedii, a company further developing these drugs. A.B. and J.D. are founders and shareholders in NuMedii.

Authors' Contributions

N.J. was responsible for the experimental design, data analysis, and the execution of most of the experiments under the guidance of J.S. J.D. performed the bioinformatics drug repositioning experiment and initial analysis under the guidance of A.B. N.F., D.Y., A.P., and K.T. helped with some cell culture experiments and quantifications. A.Z., A.P., and M.Z. helped with some experiments in mice. P.M. helped with the human primary xenografts experiments, generated the novel pancreatic neuroendocrine tumor mouse model, and performed imipramine treatment in these mice. K.K. performed the mass spectrometry data and analysis. K.P. provided the mouse SCLC cells. P.K. and D.V. helped with the bioinformatics analyses. J.W.N. and J.W.R. provided clinical advice throughout the study. N.J. and J.S. wrote most of the manuscript.

NIH-PA Author Manuscript
NIH-PA Author Manuscript
NIH-PA Author Manuscript

NIH-PA Author Manuscript

NIH-PA Author Manuscript

NIH-PA Author Manuscript

Keywords

Small Cell Lung Cancer (SCLC); drug repositioning; Tricyclic Antidepressants (TCAs); imipramine; G-protein coupled receptors (GPCRs)

Introduction

The identification of therapeutic approaches for the treatment of cancer is an arduous, costly, and often inefficient process. Drug repositioning, which is the discovery of new indications for existing drugs that are outside their original indications, is an increasingly attractive mode of therapeutic discovery. In addition to saving time and money, an advantage of drug repurposing strategies is the fact that existing drugs have already been vetted in terms of safety, dosage, and toxicity. Therefore, repurposed candidate drugs can often enter clinical trials much more rapidly than newly-developed drugs (1). Recent advancements in computing, concomitant with the dramatic expansion of available high-throughput data sets, have enabled the development of *in silico* approaches to drug discovery, including the incorporation of genomics-, network-, systems-, and signature-based approaches While these computational approaches are still in their infancy, emerging evidence suggests that they enable the discovery of novel treatment options for a wide range of human diseases (2–6).

Lung cancer is the number one cause of cancer deaths in the world, with more than 1.3 million deaths annually. Lung cancer is divided into two major histopathological groups: non-small cell lung cancer (NSCLC, ~80–85% of cases) and small cell lung cancer (SCLC, ~15–20% of cases) (7, 8). SCLC is a very deadly subtype of lung cancer characterized by the rapid expansion and metastasis of small cells with neuroendocrine features. Patients are most commonly diagnosed with metastatic (extensive stage) disease. Without treatment, they may only survive a few weeks to months after the initial diagnosis, but systemic chemotherapy improves the median survival to approach a year. Still, cure is not possible with currently employed therapies and there is no approved targeted therapy for SCLC despite numerous attempts and clinical trials (9). In the recent years, a substantial effort from many groups has been made to identify novel treatment options for SCLC. For instance, a proteomic profiling approach has recently identified PARP1 as a novel therapeutic target in SCLC (10). However, it is essential to identify additional therapeutic strategies to block the growth of SCLC tumors.

In this study, we sought to employ a systematic drug repositioning bioinformatics approach to identify novel FDA-approved candidate drugs to treat SCLC. Using this strategy, we identified tricyclic antidepressants (TCAs) and related inhibitors of G-protein coupled receptors (GPCRs) as potent inducers of cell death in SCLC cells and other neuroendocrine tumors.

Results

To identify novel therapeutic strategies for SCLC patients, we used a bioinformatics approach that evaluates the therapeutic potential of FDA-approved drugs for a given disease by comparing gene expression profiles in response to these drugs in multiple cell types across multiple diseases (4) (Fig. 1A). From this drug repositioning approach, we computed a list of candidate drugs with predicted efficacy against SCLC (Supplementary Table 1). This list contained a wide variety of drugs, including some chemotherapeutic agents previously tested with some success in SCLC patients (e.g. doxorubicin, irinotecan (7)), suggesting that these agents used in the clinic may affect the SCLC gene expression

NIH-PA Author Manuscript

NIH-PA Author Manuscript

NIH-PA Author Manuscript

signature. Rather than screen a large number of candidate drugs in cells, we first annotated the known targets of the top-scoring candidates, as well as the pathways enriched in these drug targets (Table 1). This analysis led us to focus on drugs targeting molecules in the "Neuroactive ligand receptor interaction" and "Calcium Signaling" pathways, the top two most significant pathways. Notably, SCLC cells are known to express molecules in these pathways, including neurohormonal ligands, channels, and receptors (11–13).

We selected an initial group of six drugs for experimental validation from these two groups. In the "Neuroactive ligand receptor interaction" module, imipramine and clomipramine are two first-generation tricyclic antidepressants (TCAs) with moderate to strong serotonin and epinephrine reuptake inhibition activity, which also display strong anti-cholinergic, anti-histaminic, and anti-adrenergic effects. Promethazine is a first-generation Histamine H1 receptor antagonist that also possesses anti-cholinergic and anti-adrenergic activities. Tranylcypromine and pargyline are irreversible inhibitors of the enzymes monoamine oxidase A and B, respectively. In the "Calcium signaling pathway", bepridil blocks both voltage- and receptor-operated calcium channels.

We first performed cell viability assays after exposure to the drugs in culture. As a negative control, we used the lung adenocarcinoma (NSCLC) cell lines A549 (human) and LKR13 (mouse), which are not expected to respond to the same candidate drugs (5). We tested three established human SCLC lines (H82, H69, and H187) and three primary tumor cell lines from a genetically defined mouse model of SCLC (Kp1, Kp2 and Kp3) (14). The doses and concentrations used were optimized for each drug and ranged from 1–20μM for bepridil and 10–100μM for clomipramine, promethazine, imipramine, tranylcypromine, and pargyline; all these doses have been well documented in multiple cellular contexts. We confirmed that the IC_{50} of these drugs in the human and mouse SCLC cells used was in the same ranges as was previously reported (Supplementary Fig. 1A and data not shown). Next, we used the IC_{80} of the selected drugs to determine the survival of each cell line compared to its vehicle-treated control. Treatment of SCLC cells with imipramine, clomipramine, promethazine, and bepridil, but not tranylcypromine or pargyline, significantly inhibited the growth of mouse and human SCLC but not NSCLC cells when cultured in 0.5% or 2% serum (Fig. 1B and C). Cells were also responsive to the drugs in higher serum conditions (5% and 10%, data not shown). Phase contrast images of control and treated SCLC cells suggested that imipramine, promethazine, and bepridil were inducing cell death rather than having cytostatic effects (Supplementary Fig. 1B). Of note, the least responsive SCLC cell line in this initial analysis, H82 cells, are often classified as a variant SCLC cell line with decreased neuroendocrine features.

Based on these experiments in culture, we selected one drug in each of the three main categories to perform experiments *in vivo* (imipramine, promethazine, and bepridil). Once measurable tumors had formed after subcutaneous injection of SCLC cells in immunocompromised NSG mice, we treated the transplanted mice for 2 weeks daily with each drug (Fig. 2A). All three drugs inhibited the growth of transplanted mouse Kp1 and Kp3 SCLC cells and human H187 SCLC cells as single agents, although the effects of bepridil were not as significant on the human cell line (Fig. 2B and C and data not shown); promethazine inhibited the growth of human H82 SCLC xenografts significantly, while imipramine had a less profound effect (data not shown). We next treated a human primary SCLC tumor growing under the skin of NSG mice with imipramine or promethazine (Fig. 2D) and found that the two drugs had a long-term cytostatic effect on tumor growth (Fig. 2D and E).

These results led us to further investigate the effects and mechanisms of action of the two best candidate drugs, the tricyclic anti-depressant imipramine and the anti-histamine and

NIH-PA Author Manuscript

NIH-PA Author Manuscript

NIH-PA Author Manuscript

anti-emetic promethazine. To determine the efficacy of the candidate drugs on primary tumors *in vivo*, we examined how endogenous SCLC tumors developing in the lungs of *Rb/p53/p130* mutant mice (15) responded to drug treatment. Five months after intra-tracheal instillation of Ad-Cre to delete the three tumor suppressor genes and initiate tumor development, at a time when these mutant mice have developed advanced lesions, daily intra-peritoneal (IP) injections of imipramine, promethazine, or saline were performed on groups of mutant mice. After 30 days of treatment (Fig. 3A), the analysis of whole lungs and hematoxylin and eosin-stained sections indicated that imipramine- and promethazine-treated mice had fewer and smaller SCLC tumors than control mice (Fig. 3B). Drug treatment significantly reduced tumor burden as measured by the total tumor area occupying the lungs and the size of the tumors (Fig. 3C and D). Three out of ten control mice developed large metastases in their liver, as described before (15), while no large lesions were found in the six promethazine-treated and nine imipramine-treated mice analyzed.

SCLC patients are typically treated with a combination of a platinum-based agent and etoposide. Patients often respond well initially but almost invariably relapse with disease that is often resistant to their primary therapy and other agents (9). We observed strong toxicity in tumor-bearing mice simultaneously treated with both cisplatin and etoposide (data not shown), limiting our ability to assess the long-term response of endogenous tumors to both drugs. Consequently, to determine the effects of the candidate drugs on chemoresistant tumors, we treated *Rb/p53/p130;Rosa26*$^{LSL\text{-}Luciferase}$ mutant mice bearing SCLC tumors with saline or cisplatin only, using luciferase expression to monitor tumor burden *in vivo* (Fig. 3E). Tumors that had survived chemotherapy and control chemonaïve tumors (Fig. 3F) were then grown in culture or transplanted into immunocompromised recipient mice (Fig. 3E). We found that chemoresistant mouse tumors were inhibited by imipramine treatment similar to chemonaïve tumors both *ex vivo* (data not shown) and in primary allografts (Fig. 3G and H). Thus, tumor cells emerging from long-term treatment with a chemotherapeutic agent are still inhibited by this candidate drug.

Together, these experiments indicate that the expansion of SCLC cells is potently inhibited by imipramine and promethazine and suggest that both chemoresistant tumors and disseminated tumors may respond to treatment in patients with advanced disease.

The visual appearance of SCLC cells treated with imipramine and promethazine in culture suggested that these drugs inhibit SCLC growth by inducing cell death (Supplementary Fig. 1B). Indeed, we found that drug treatment led to apoptotic cell death in culture (data from two representative cell lines, mouse Kp1 cells and human H82 cells), in transplanted tumors, and in endogenous mouse tumors (Fig. 4A, Supplementary Fig. 2A and B, and Fig. 4B and C, respectively). A concomitant decrease in proliferation was also observed in tumor sections *in vivo* (Supplementary Fig. 2C). Importantly, treatment with the pan-Caspase inhibitor zVAD-FMK rescued the cell death induced by imipramine after 24 hours in a dose-dependent manner (Fig. 4D and E), further indicating that apoptotic cell death is a major mechanism by which the candidate drugs inhibit SCLC growth. No induction of cell death was observed in human A549 and mouse LKR13 NSCLC cells in culture at the drug concentrations used (Fig. 1C, Supplementary Fig. 1B, and data not shown) or in the lung epithelium of mice treated daily for one month with the candidate drugs, including lung neuroendocrine cells (Supplementary Fig. 2D). We also noted large areas of necrosis in treated tumors (Supplementary Fig. 2B) and found that treatment of SCLC cells with an inhibitor of necrosis also partly rescued the cell death induced by the candidate drugs in culture (Supplementary Fig. 2E). Thus, the candidate drugs induce a rapid cell death specifically in neuroendocrine tumor cells.

NIH-PA Author Manuscript

NIH-PA Author Manuscript

NIH-PA Author Manuscript

Washing out the drugs up to 6 hours after addition to the cells was enough to prevent the appearance of cell death and the decrease in viability observed 24 hours after treatment, while exposure of the cells to imipramine for 8 hours or more was sufficient to induce an irreversible cell death in SCLC cells (Supplementary Fig. 3A). This observation allowed us to begin to explore the signaling mechanisms downstream of imipramine treatment in SCLC cells (16, 17). Because the calcium channel blocker bepridil had also some inhibitory effect on SCLC cells (Fig. 1 and Supplementary Fig. 1), we examined changes in calcium levels in response to imipramine and promethazine. We observed a rapid decrease in intracellular calcium levels in SCLC cells after treatment with both drugs (Fig. 4F and Supplementary Fig. 3B and C). We also observed increased levels of reactive oxygen species (ROS) after drug treatment (Supplementary Fig. 3D). Increased ROS and oscillations in calcium levels have been directly linked to activation of Caspases and apoptotic cell death in certain contexts, including *via* activation of stress MAPK pathways (18). Accordingly, we found changes in the JNK/c-Jun pathway upon treatment of SCLC cells with imipramine starting at 1 hour after treatment (Fig. 4G). This rapid activation of the stress MAPK pathway was only detected in SCLC cells and not in mouse or human NSCLC cells (Fig. 4H). Combined treatment of SCLC cells with imipramine and the selective JNK inhibitor SP600125 resulted in a significant rescue of the cell death induced by imipramine (Fig. 4I). Together, these experiments indicate that treatment of SCLC cells with the candidate drugs triggers cellular stresses culminating in apoptotic and necrotic cell death.

The variety of responses triggered by imipramine and promethazine and their known binding to multiple receptors at the surface of cells makes it very likely that one reason they are so effective at inducing death in SCLC is their action on multiple targets. This broad range of action of the candidate drugs may be a positive aspect clinically. Nevertheless, we sought to identify at least some of the molecules targeted by these drugs in SCLC. Based on previous pharmacological studies (19, 20), the dose of imipramine that we used in mice is in the same range as the dose to treat depression in patients, suggesting that the candidate drugs act at least in part through the targets for which they have the highest affinity, including the histamine H1 receptor (H1R), the muscarinic Acetylcholine receptor (mAchR, including the CHRM3 isoform), the 5-HT2 Serotonin receptor (HTR2, and in particular HTR2a), and the alpha1-adrenergic receptor (ADRA1a and ADRA1b) (21–26). Our analysis of microarray experiments from human (27–29) and mouse (15) SCLC, binding assays, and previous reports (30–32), all indicate that these GPCRs are expressed in SCLC cells (Supplementary Fig. 4A and B). These observations led us to treat SCLC cells with related molecules and selective inhibitors of these GPCRs; we also ectopically added purified ligands. Treatment with amitriptyline and desipramine, two first-generation TCAs with high binding affinity to H1R, HTR2, ADRA1, and mAchR, doxazosin mesylate (a selective ADRA1 antagonist), azelastine (H1R), 4-DAMP (CHRM3), and ritanserin (HTR2), in all cases led to a significant reduction in cell survival specifically in SCLC cells and not in NSCLC cells (Fig. 5A and Supplementary Fig. 5A–E). Furthermore, addition of purified epinephrine and of a selective agonist of the H1R to the culture medium was sufficient to increase survival and partially rescued the cell death phenotype induced by promethazine and imipramine (Fig. 5B and Supplementary Fig. 5F). Acetylcholine and serotonin also partially rescued the cell death induced by promethazine, which possesses fewer targets than imipramine (Supplementary Fig. 5G and H). Importantly, SCLC cells express the enzymes required for the biosynthesis of the ligands that normally activate the main GPCRs inhibited by this drug (Supplementary Fig. 6A). We also detected the rapid production of serotonin and epinephrine in the supernatant of SCLC cells by mass spectrometry (Supplementary Fig. 6B and C). Of note, competition by these endogenous ligands may explain the relatively high concentrations of drugs required to induce cell death in SCLC cells.

NIH-PA Author Manuscript

NIH-PA Author Manuscript

NIH-PA Author Manuscript

Different GPCRs often activate similar downstream signaling pathways, including the $G\alpha_s$ adenyl cyclase (AC)/cAMP/protein kinase A (PKA) module, and the $G\alpha_q$ phospholipase C beta (PLCβ)/protein kinase c (PKC) module (33, 34). Our analysis of microarray experiments indicated that most of the different Gα subunits are expressed in SCLC cells, including the $G\alpha_s$ and $G\alpha_q$ subunits (Supplementary Fig. 7A). H1R, CHRM3, ADRA1 and HTR2A are usually thought to be $G\alpha_q$ -coupled receptors (26, 35–37), which led us to first test whether blocking PKC signaling may reduce the survival of SCLC cells. However, treatment with the PKC inhibitor GF109203X had no significant inhibitory effect on the survival of mouse and human SCLC cells (Fig. 5C). In addition, treatment with the PKC activator phorbol 12-myristate 13-acetate (PMA) did not rescue the cell death induced by imipramine (Fig. 5D). Accordingly, we did not observe any decrease in phospho-PKC levels (an indicator of PKC activation) at different time points after imipramine treatment in SCLC cells (Fig. 5E and data not shown).

Some reports suggest that, in certain contexts, the GPCRs targeted by the candidate drugs can also signal through $G\alpha_s$ signaling, leading to an increase in adenyl cyclase activity, cAMP levels, PKA activity, and ultimately CREB (38–42). Thus, we next tested the alternative possibility that imipramine and promethazine may induce cell death in SCLC cells by interfering with $G\alpha_s$ signaling. Indeed, we observed a decrease in the phosphorylation of the PKA substrates CREB and ATF1 starting at 30 minutes after imipramine treatment in SCLC cells (Fig. 5E and data not shown). To determine the involvement of the $G\alpha_s$ signaling pathway in the survival of SCLC cells and in response to the TCAs, we first treated the cells with inhibitors of this pathway. Treatment with KH7 (an inhibitor of soluble adenyl cyclase) and H-89 dihydrochloride (an inhibitor of PKA) decreased the survival of SCLC cells, but not of NSCLC cells, in a dose-dependent manner (Fig. 5F and G). We next used forskolin and the phosphodiesterase inhibitor 3-isobutyl-1-methylxanthine (IBMX), which activate adenyl cyclase and raise the levels of intracellular cAMP, leading to subsequent PKA activation. Upon addition of forskolin and/or IBMX, alone or in combination, to vehicle-treated mouse and human SCLC cells, no significant increase in cell viability was observed after 24 hours (Fig. 5H). In contrast, addition of 50μM of forskolin alone or 100μM of IBMX alone to imipramine-treated SCLC cells, partially rescued the cell death phenotype; full rescue of viability was observed when forskolin and IBMX were added together (Fig. 5I). Finally, the addition of forskolin and IBMX to imipramine-treated cells reverted the elevated levels of phospho-c-Jun to the levels observed in untreated cells (Fig. 5J). These results indicate that imipramine and promethazine induce cell death of SCLC cells by affecting signaling downstream of the $G\alpha_s$ subunit of the targeted GPCRs, thereby inhibiting the adenyl cyclase and cAMP-dependent activation of PKA and inducing cell death *via* activation of the JNK/c-Jun module (43).

While the candidate drugs probably bind to multiple targets in SCLC cells, these experiments suggest that the potent effects of these drugs in the induction of cell death in SCLC cell populations are mediated at least in part by the capacity of these drugs to disrupt autocrine survival loops between neurotransmitters and their receptors at the surface of SCLC cells. These observations in SCLC led us to hypothesize that other neuroendocrine tumors may have similar signaling networks as SCLC cells and may be sensitive to the same drugs. The analysis of the few publicly available microarray experiments from other rare human neuroendocrine tumors indicates that Merkel cell carcinoma, midgut carcinoid tumors, pheochromocytoma, and neuroblastoma tumor cells also express several of the main GPCR targets of imipramine and promethazine (Fig. 6A). Indeed, we found that both drugs are efficient in inducing rapid cell death in human cell lines from most of these cancer types as well as in mouse pancreatic neuroendocrine tumor cells, but not as strongly and efficiently as in non-neuroendocrine pancreatic adenocarcinoma cells (Supplementary Fig. 7B and Fig. 6B and C). We also tested neuroendocrine Large Cell Carcinoma cells and

NIH-PA Author Manuscript

NIH-PA Author Manuscript

NIH-PA Author Manuscript

Large Cell Lung adenocarcinoma cells and found that they do not undergo significant cell death in response to both imipramine and promethazine (Supplementary Fig. 7B and Fig. 6B and C). We recently developed a novel model of pancreatic neuroendocrine tumors resulting from the deletion of *Rb*, *p53*, and *p130* in insulin-producing cells (*RIP-Cre Rb/p53/p130*, similar to the RIP-Tag model (44)). These mice develop pancreatic tumors expressing insulin (Fig. 6D) and die approximately two months after birth (Fig. 6E). We found that treatment of these mice with imipramine starting at day 35 significantly increased survival (from 58 days for the mice injected with saline to 74.5 days for imipramine treated mice, p=0.024), further validating imipramine as a novel therapeutic agent against neuroendocrine tumors (Fig. 6E).

Discussion

In this study, we used a systematic computational drug repositioning strategy to identify FDA-approved tricyclic antidepressants (TCAs) and related molecules as potent inducers of cell death in SCLC cells through activation of stress pathways. We also show that the same drugs induce cell death in other types of neuroendocrine tumor cells. Together, these experiments elucidate a general mechanism of survival in neuroendocrine tumor cells and identify a common therapeutic strategy for a heterogeneous group of cancer patients.

Our observations linking the survival of SCLC cells to the activity of GPCRs may be relevant to the biology of other tumors, including brain tumors as suggested by epidemiological studies (45), retinoblastoma (46), and pancreatic neuroendocrine tumors (47), which can be inhibited by drugs targeting neuronal signaling such as monoamine transmitters and receptors. Our study also illustrates the potential of drug repositioning approaches, especially computational approaches, in the treatment of cancer. In this specific case, we were able to experimentally expand our findings in SCLC to other neuroendocrine tumors for which few gene expression profile datasets exist and for which the bioinformatics pipeline would not have been possible.

Our experiments suggest that inhibition of GPCRs at the surface of SCLC cells results in inhibition of PKA activity. An important aspect of future experiments will be to continue to investigate the signaling networks perturbed by these drugs in SCLC cells. We found that one important difference between SCLC and NSCLC cells is the rapid activation of the stress MAPK pathway in response to the candidate drugs. Thus, it will be interesting to determine if the engagement of different Gα subunits and downstream effectors explains the sensitivity of neuroendocrine cancer cells to these drugs. On a related note, we did not find a significant correlation between the mRNA expression levels of the candidate GPCRs and drug response in cancer cells. In particular, adenocarcinoma cells and other normal cells express these GPCRs at levels similar to SCLC cells, but do not die in response to the same drugs. It is probable that the total levels of these GPCRs on the surface of SCLC cells are not the determinant of the drug response but rather it is the activity of the molecular components of the signaling pathway downstream of the GPCRs and/or the activity of the ligands secreted by SCLC cells. Similar observations have been made recently in lung adenocarcinoma cells in which the effects of EGFR inhibition are not dependent on EGFR levels (48). Future experiments will be needed to shed light into the establishment of autocrine survival loops between GPCRs and their ligands in SCLC cells and to determine how these loops promote the survival of SCLC cells.

We have made a substantial effort to identify patients that may have been treated with TCAs incidentally as part of their routine care. Promethazine is sometimes used for nausea, but its heavily sedating effects limits its outpatient use to infrequent use, and much more commonly the preferred phenothiazine antiemetic drug is prochlorperazine, as it is much

NIH-PA Author Manuscript

NIH-PA Author Manuscript

NIH-PA Author Manuscript

less sedating. Even this drug is only received intermittently for the primary prevention of nausea from cisplatin and other chemotherapies. We have searched the electronic portion of the Stanford medical record (dating back around year 2000) for patients who received a TCA and found less than 5, none of whom were on the drugs chronically. Similarly, other databases searches did not yield high patient numbers. Based on our pre-clinical results, prospective validation of these findings in a clinical trial setting has begun (NCT01719861 – A Phase IIa Trial of Desipramine in Small Cell Lung Cancer and Other High-Grade Neuroendocrine Tumors), but reportable results are not expected for years. An advantage of a drug repositioning approach with approved medications for other indications is accelerated drug development times.

TCAs have been largely replaced in the clinic by a new generation of selective Serotonin reuptake inhibitors (SSRIs). However, the anti-cancer effects of TCAs are in large part due to the less specific, “off-target” mode of action of these drugs, which target multiple molecules at the surface of cells. Monoamine oxidase inhibitors, tranylcypromine and pargyline, do not antagonize these GPCRs and are not efficient in inducing cell death in SCLC cells. The fact that TCAs target multiple surface molecules has important consequences for cancer patients: first, our analysis of gene expression profiles of SCLC and other neuroendocrine tumors indicate that most, if not all individual tumors express at least one of these GPCRs. Thus, the vast majority of neuroendocrine tumors may be at least partly responsive to TCA treatment. In addition, acquired resistance to TCA treatment may take a long time to occur. Additional experiments in pre-clinical mouse models and early phase clinical trials in patients with these FDA-approved drugs may help rapidly identify ways to translate these observations to better treatment options for patients with neuroendocrine tumors.

Finally, we believe that imipramine and other related TCAs could be potentially used as a second-line therapy on SCLC patients who become refractory to cisplatin/etoposide. Our studies indicate that cisplatin-resistant tumors are still sensitive to imipramine treatment. We have tested the effects of combining imipramine with cisplatin at the early stages when the tumor was still sensitive to cisplatin *in vivo*, but we did not observe a significant greater decrease in tumor growth compared to imipramine alone or cisplatin alone at the concentrations used; both drugs induce apoptotic cell death and may not induce more death together (data not shown). Moreover, the side effect profile of TCAs is not benign and combining with chemotherapy will likely substantially increase toxicity in a patient population with often compromised functional status, further reducing potential clinical benefit. Based on these observations, we propose that TCAs in the platinum refractory setting or as maintenance treatment after chemotherapy may be the most useful settings for these candidate drugs in clinical trials.

Methods

Ethics statement

Mice were maintained according to practices prescribed by the NIH at Stanford’s Research Animal Facility accredited by the AAPLAC.

Drug repositioning and bioinformatics approach

The drug repositioning analysis was based on a systematic approach described previously (4, 5). Detailed information can be found in the supplementary data section.

NIH-PA Author Manuscript

NIH-PA Author Manuscript

NIH-PA Author Manuscript

Mice, adenoviral infections, and subcutaneous xenografts

The SCLC mouse model bearing deletions in *p53*, *Rb*, and *p130* (TKO) was previously described (15). The pancreatic neuroendocrine cancer mouse model is based on the deletion of *Rb*, *p53*, and *p130* in insulin-producing cells (*RIP-Cre Rb/p53/p130*, similar to the RIP-Tag model (44)). This mouse model will be described in detail somewhere else. Ad-Cre (Baylor College of Medicine) infections were performed as previously described (14). Mice were maintained at the Stanford Research Animal Facility accredited by the Association for Assessment and Accreditation of Laboratory Animal Care. NOD.SCID.Gamma mice were housed in the barrier facility at Stanford University. For the endogenous SCLC mice, treatment started 5 months after Ad-Cre infection. Imipramine (25mg/kg), promethazine (25mg/kg), and bepridil (10mg/kg) were administrated intraperitoneally daily for 30 consecutive days, while cisplatin (5mg/kg) was administrated intraperitoneally once weekly for a total of 6–8 weeks until tumors became chemoresistant.

Chemonaïve tumors were generated after weekly injection of saline for a total of 6 weeks. Growth of these endogenous mouse tumors was monitored weekly by live imaging using Xenogen IVIS in the animal imaging facility at Stanford University and quantification of the luciferase activity was calculated using the Living imaging software. For subcutaneous injections, 0.5×10^6 mSCLC (Kp1, Kp3, saline-treated chemonaïve and cisplatin-treated chemoresistant), and 2×10^6 hSCLC (H187 and H82) cells were injected into the two flanks of each NSG mice with Matrigel (1:1) (BD Biosciences). Treatment with the drugs started once the SCLC tumors reached 100–150 mm^3 (around 10–14 days after implantation). Imipramine (25mg/kg), promethazine (25mg/kg), and bepridil (10mg/kg) were administrated intraperitoneally daily for 36–48 consecutive days. Tumor volume was measured at the times indicated and calculated using the ellipsoid formula (length × $width^2$). The human primary SCLC sample was obtained from the NDRI program at the NIH. The tumor was digested with collagenase and dispase (Roche). Cells were collected and passed through a MACS magnetic beads column to deplete $CD45^+$ blood cells. The remaining cells were injected into the flank of NSG mice with Matrigel (1:1) for expansion. Single cell suspensions (1×10^6 and 3×10^6) from this new primary cell line (NJH29) were used for the primary human xenografts studies. Treatment with the drugs started once the xenografts reached 100–150 mm^3. Saline, imipramine (25mg/Kg), and promethazine (25mg/Kg) were administrated intraperitoneally daily for 24 consecutive days.

Drugs and inhibitors

Imipramine, promethazine, clomipramine, bepridil, necrostatin-1, azelastine, epinephrine, acetylcholine, serotonin, the histamine analogue 2-(2-Pyridyl) ethylamine, forskolin, and IBMX were all purchased from Sigma Aldrich, MO. Z-VAD-FMK, ritanserin, 4-DAMP, doxazosin mesylate, H89 dihydrochloride, KH7, and GF109203X were all purchased from Tocris Bioscience, UK. The JNK inhibitor SP600125 was purchased from LC Laboratories, MA. Fluo-3AM was purchased from Invitrogen. All these powders were dissolved in the appropriate solvent according to the manufacturer's instructions.

Cell lines and tissue culture

Mouse SCLC cells (Kp1, Kp2, and Kp3) were grown in RPMI 1640 media containing 10% bovine growth serum (BGS, Fisher Scientifics) (15) or dialyzed fetal bovine serum (dFBS, Fisher Scientifics). NCI-H82, NCI-H69, and NCI-H187 human SCLC cells (ATCC) and cultured in RPMI media containing 10% serum. For the original cellular assays, we used the H82 cells because they grow very rapidly and enough cells can be obtained to perform most of these assays. However, because they are the least sensitive of all three human SCLC cell lines, we used the other cell lines in the subsequent mechanistic experiments to investigate the mechanism of action of the drugs. The NSCLC cell lines A549 and LKR13 were a

NIH-PA Author Manuscript

NIH-PA Author Manuscript

NIH-PA Author Manuscript

generous gift from the Sweet-Cordero lab. The NE-LCLC cell line H1155 was a generous gift from the Minna lab. Human pancreatic adenocarcinoma cell line PANC1, human neuroblastoma cell line HTB1, and LCLC NCI-1915 were obtained from ATCC and cultured in the same conditions as described above. The Merkel cell carcinoma cell line was a generous gift from Dr. Paul Nghiem. The neuroendocrine mouse pancreatic cancer cells (MIN-6 and β-TC, both insulinomas) were a generous gift from Dr. Seung Kim and were cultured in DMEM containing high glucose (Thermo Scientific) and 15% serum. All mouse SCLC cell lines were generated in the Sage lab and were authenticated by genotyping for the mutant alleles and the expression of neuroendocrine markers. All human cell lines were either repurchased from ATCC or given to us by other laboratories, except for NJH29, which were generated in the Sage lab; no further authentication was performed on these cell lines.

MTT assays and Calcium measurement

For 3-(4,5-dimethylthiazol-2-yl)-2,5-diphenyltetrazolium bromide (MTT) assays (Roche), floating cells were seeded at 8×10^4 (2% serum) or 1×10^5 (0.5% serum) per well in 96-well plates at day 0 and drugs were added on day 1. MTT reagents 1 and 2 were added on day 2 or day 3 depending on the experiments. The percentage survival was determined as the ratio of treated cells versus vehicle control. For all the rescue experiments, cells were pre-treated with the various drugs or exogenous ligands for 30 minutes before addition of imipramine or promethazine. Calcium measurements using the indicator Fluo3-AM were performed per the manufacturer's instructions (Invitrogen). Briefly, trypsinized cells treated with the drugs in 2% serum at different time points were stained with 2.5μM Fluo-3AM for 30 minutes in RPMI media at 37 °C. Cells were then washed in indicator free RPMI media and then resuspended in PBS directly before running them through an Aria Analyzer FACS machine.

Immunoblot analysis and immunostaining

For immunoblotting, SCLC cells were homogenized using lysis buffer containing 1% NP40, 50mM HEPES-KOH pH 7.8, 150mM NaCl, 10mM EDTA and a cocktail of protease inhibitors. The antibodies used were phospho-SAPK/JNK Thr183 and Tyr185 (p-JNK), JNK, phospho-c-Jun Ser63 (p-c-Jun), c-Jun, phospho-CREB Ser133 (p-CREB antibody also recognizes p-ATF1), CREB, pan phospho-PKC βII Ser660 (p-PKC), PKC, and cleaved Caspase 3 (all purchased from Cell signaling), Karyopherin β1 (Santa Cruz), and α-Tubulin (Sigma). We used 5μm paraffin sections for H&E staining and immunostaining. Paraffin sections were de-waxed and rehydrated in the Trilogy reagent (Cell Marque). The primary antibodies used were phospho-histone 3 Ser10 (PH3; Millipore), Cleaved Caspase 3 (CC3; Cell signaling), Insulin (DAKO), and Synaptophysin (SYN; Neuromics). Alexa Fluor secondary antibodies (Invitrogen) were used for antibody detection. Fluorescent images were captured on the Leica fluorescent microscope. For quantification of the number of CC3 and PH3 positive cells, tumor of similar size and area ranging between 1000 to 30,000 pixel units were included. Very small and very large tumors of area measuring below or above this range were excluded.

Image analysis and statistics

Analysis of tumor areas and fluorescent images was done using ImageJ software by measuring pixel units. Mice were scored as having significant liver metastases if they had more than 3 metastases with at least 50 cells each. Statistical significance was assayed by Student's t test with the Prism GraphPad software (two-tailed unpaired and paired t-test depending on the experiment). *: p-value<0.05; **: p-value<0.01; ***: p-value<0.005; ns: not significant. Data are represented as mean +/− standard error of the mean. For the survival curve analysis and comparison, we used the Mantel-Cox test.

NIH-PA Author Manuscript

NIH-PA Author Manuscript

NIH-PA Author Manuscript

Supplementary Material

Refer to Web version on PubMed Central for supplementary material.

Acknowledgments

We would like to thank Dr. Anton Berns for the *Trp53*^{lox} mice, Dr. Luis Parada for helpful comments, the Sweet-Cordero lab for suggestions throughout the project, cell lines, and antibodies, Dr. Brian Kobilka and Dr. Pawel Niewiadomski for helpful discussions on GPCR signaling, Andrew Kruse for performing the binding assay to measure the number of mAchR, Dr. Paul Nghiem for the MCC cell line, Dr. Seung Kim for the pancreatic neuroendocrine cell lines, Alex Augustyn and Dr. John Minna for the neuroendocrine large cell lung cancer cell lines, and members of the Sage lab for their help throughout the course of this study.

Financial Support: This work was supported by the Lucile Packard Foundation for Children's Health (J.S.), the Department of the Army (W81XWH-13-1-0211, J.S.), the NLM Biomedical Informatics Training Grant (T15 LM007033) to Stanford University (J.T.D.), the National Cancer Institute (5R01CA138256-04, A.J.B. and J.S.), the Stanford Dean's Fellowship and NRSA T32 Academic Research Training in Pulmonary Medicine and a California TRDRP post-doctoral fellowship (N.J.), and a Stanford Cancer Institute Developmental Cancer Research award (J.N. and J.R.)

References

1. Ashburn TT, Thor KB. Drug repositioning: identifying and developing new uses for existing drugs. Nature reviews Drug discovery. 2004; 3:673–83.
2. Li YY, An J, Jones SJ. A computational approach to finding novel targets for existing drugs. PLoS Comput Biol. 2011; 7:e1002139. [PubMed: 21909252]
3. Yang L, Agarwal P. Systematic drug repositioning based on clinical side-effects. PLoS ONE. 2011; 6:e28025. [PubMed: 22205936]
4. Dudley JT, Sirota M, Shenoy M, Pai RK, Roedder S, Chiang AP, et al. Computational repositioning of the anticonvulsant topiramate for inflammatory bowel disease. Sci Transl Med. 2011; 3:96ra76.
5. Sirota M, Dudley JT, Kim J, Chiang AP, Morgan AA, Sweet-Cordero A, et al. Discovery and preclinical validation of drug indications using compendia of public gene expression data. Sci Transl Med. 2011; 3:96ra77.
6. Cheng F, Liu C, Jiang J, Lu W, Li W, Liu G, et al. Prediction of Drug-Target Interactions and Drug Repositioning via Network-Based Inference. PLoS Comput Biol. 2012; 8:e1002503. [PubMed: 22589709]
7. van Meerbeeck JP, Fennell DA, De Ruysscher DK. Small-cell lung cancer. Lancet. 2011; 378:1741–55. [PubMed: 21565397]
8. Heist RS, Engelman JA. SnapShot: non-small cell lung cancer. Cancer Cell. 2012; 21:448, e2. [PubMed: 22439939]
9. Neal JW, Gubens MA, Wakelee HA. Current management of small cell lung cancer. Clin Chest Med. 2011; 32:853–63. [PubMed: 22054891]
10. Byers LA, Wang J, Nilsson MB, Fujimoto J, Saintigny P, Yordy J, et al. Proteomic profiling identifies dysregulated pathways in small cell lung cancer and novel therapeutic targets including PARP1. Cancer Discov. 2012; 2:798–811. [PubMed: 22961666]
11. Wistuba, Gazdar AF, Minna JD. Molecular genetics of small cell lung carcinoma. Seminars in oncology. 2001; 28:3–13. [PubMed: 11479891]
12. Moody TW, Chan D, Fahrenkrug J, Jensen RT. Neuropeptides as autocrine growth factors in cancer cells. Current pharmaceutical design. 2003; 9:495–509. [PubMed: 12570813]
13. Onganer PU, Seckl MJ, Djamgoz MB. Neuronal characteristics of small-cell lung cancer. British journal of cancer. 2005; 93:1197–201. [PubMed: 16265346]
14. Park KS, Martelotto LG, Peifer M, Sos ML, Karnezis AN, Mahjoub MR, et al. A crucial requirement for Hedgehog signaling in small cell lung cancer. Nat Med. 2011; 17:1504–8. [PubMed: 21983857]

NIH-PA Author Manuscript

NIH-PA Author Manuscript

NIH-PA Author Manuscript

15. Schaffer BE, Park KS, Yiu G, Conklin JF, Lin C, Burkhart DL, et al. Loss of p130 accelerates tumor development in a mouse model for human small-cell lung carcinoma. Cancer Res. 2010; 70:3877–83. [PubMed: 20406986]
16. Kiselyov K, Shin DM, Muallem S. Signalling specificity in GPCR-dependent Ca2+ signalling. Cellular signalling. 2003; 15:243–53. [PubMed: 12531423]
17. Thompson MD, Burnham WM, Cole DE. The G protein-coupled receptors: pharmacogenetics and disease. Critical reviews in clinical laboratory sciences. 2005; 42:311–92. [PubMed: 16281738]
18. Berridge MJ, Lipp P, Bootman MD. The versatility and universality of calcium signalling. Nature reviews Molecular cell biology. 2000; 1:11–21.
19. Perry PJ, Zeilmann C, Arndt S. Tricyclic antidepressant concentrations in plasma: an estimate of their sensitivity and specificity as a predictor of response. Journal of clinical psychopharmacology. 1994; 14:230–40. [PubMed: 7962678]
20. Fisar Z, Krulik R, Fuksova K, Sikora J. Imipramine distribution among red blood cells, plasma and brain tissue. General physiology and biophysics. 1996; 15:51–64. [PubMed: 8902557]
21. Petersen RC, Richelson E. Anticholinergic activity of imipramine and some analogs at muscarinic receptors of cultured mouse neuroblastoma cells. Psychopharmacology. 1982; 76:26–8. [PubMed: 6281837]
22. Chen G, Hasanat KA, Bebchuk JM, Moore GJ, Glitz D, Manji HK. Regulation of signal transduction pathways and gene expression by mood stabilizers and antidepressants. Psychosomatic medicine. 1999; 61:599–617. [PubMed: 10511011]
23. Assanasen P, Naclerio RM. Antiallergic anti-inflammatory effects of H1-antihistamines in humans. Clinical allergy and immunology. 2002; 17:101–39. [PubMed: 12113215]
24. Donati RJ, Rasenick MM. G protein signaling and the molecular basis of antidepressant action. Life sciences. 2003; 73:1–17. [PubMed: 12726882]
25. Lopez-Munoz F, Alamo C. Monoaminergic neurotransmission: the history of the discovery of antidepressants from 1950s until today. Current pharmaceutical design. 2009; 15:1563–86. [PubMed: 19442174]
26. Fribourg M, Moreno JL, Holloway T, Provasi D, Baki L, Mahajan R, et al. Decoding the Signaling of a GPCR Heteromeric Complex Reveals a Unifying Mechanism of Action of Antipsychotic Drugs. Cell. 2011; 147:1011–23. [PubMed: 22118459]
27. Bhattacharjee A, Richards WG, Staunton J, Li C, Monti S, Vasa P, et al. Classification of human lung carcinomas by mRNA expression profiling reveals distinct adenocarcinoma subclasses. Proceedings of the National Academy of Sciences of the United States of America. 2001; 98:13790–5. [PubMed: 11707567]
28. Rohrbeck A, Neukirchen J, Rosskopf M, Pardillos GG, Geddert H, Schwalen A, et al. Gene expression profiling for molecular distinction and characterization of laser captured primary lung cancers. Journal of translational medicine. 2008; 6:69. [PubMed: 18992152]
29. Greshock J, Bachman KE, Degenhardt YY, Jing J, Wen YH, Eastman S, et al. Molecular target class is predictive of in vitro response profile. Cancer Res. 2010; 70:3677–86. [PubMed: 20406975]
30. Heasley LE. Autocrine and paracrine signaling through neuropeptide receptors in human cancer. Oncogene. 2001; 20:1563–9. [PubMed: 11313903]
31. Song P, Sekhon HS, Lu A, Arredondo J, Sauer D, Gravett C, et al. M3 muscarinic receptor antagonists inhibit small cell lung carcinoma growth and mitogen-activated protein kinase phosphorylation induced by acetylcholine secretion. Cancer Res. 2007; 67:3936–44. [PubMed: 17440109]
32. Zhang S, Togo S, Minakata K, Gu T, Ohashi R, Tajima K, et al. Distinct roles of cholinergic receptors in small cell lung cancer cells. Anticancer research. 2010; 30:97–106. [PubMed: 20150622]
33. Rasenick MM, Chaney KA, Chen J. G protein-mediated signal transduction as a target of antidepressant and antibipolar drug action: evidence from model systems. J Clin Psychiatry. 1996; 57 (Suppl 13):49–55. discussion 6–8. [PubMed: 8970504]
34. Donati RJ, Rasenick MM. G protein signaling and the molecular basis of antidepressant action. Life Sci. 2003; 73:1–17. [PubMed: 12726882]

NIH-PA Author Manuscript

NIH-PA Author Manuscript

NIH-PA Author Manuscript

35. Hill SJ. Distribution, properties, and functional characteristics of three classes of histamine receptor. Pharmacol Rev. 1990; 42:45–83. [PubMed: 2164693]
36. Billington CK, Penn RB. m3 muscarinic acetylcholine receptor regulation in the airway. Am J Respir Cell Mol Biol. 2002; 26:269–72. [PubMed: 11867333]
37. Chen ZJ, Minneman KP. Recent progress in alpha1-adrenergic receptor research. Acta Pharmacol Sin. 2005; 26:1281–7. [PubMed: 16225747]
38. Traish AM, Moreland RB, Gallant C, Huang YH, Goldstein I. G-protein-coupled receptor agonists augment adenylyl cyclase activity induced by forskolin in human corpus cavernosum smooth muscle cells. Recept Signal Transduct. 1997; 7:121–32. [PubMed: 9392440]
39. Lonze BE, Ginty DD. Function and regulation of CREB family transcription factors in the nervous system. Neuron. 2002; 35:605–23. [PubMed: 12194863]
40. Shinoura H, Shibata K, Hirasawa A, Tanoue A, Hashimoto K, Tsujimoto G. Key amino acids for differential coupling of alpha1-adrenergic receptor subtypes to Gs. Biochem Biophys Res Commun. 2002; 299:142–7. [PubMed: 12435400]
41. Moniri NH, Booth RG. Role of PKA and PKC in histamine H1 receptor-mediated activation of catecholamine neurotransmitter synthesis. Neurosci Lett. 2006; 407:249–53. [PubMed: 16978782]
42. Schroder R, Janssen N, Schmidt J, Kebig A, Merten N, Hennen S, et al. Deconvolution of complex G protein-coupled receptor signaling in live cells using dynamic mass redistribution measurements. Nat Biotechnol. 2010; 28:943–9. [PubMed: 20711173]
43. Gerits N, Kostenko S, Shiryaev A, Johannessen M, Moens U. Relations between the mitogen-activated protein kinase and the cAMP-dependent protein kinase pathways: comradeship and hostility. Cell Signal. 2008; 20:1592–607. [PubMed: 18423978]
44. Hanahan D. Heritable formation of pancreatic beta-cell tumours in transgenic mice expressing recombinant insulin/simian virus 40 oncogenes. Nature. 1985; 315:115–22. [PubMed: 2986015]
45. Walker AJ, Card T, Bates TE, Muir K. Tricyclic antidepressants and the incidence of certain cancers: a study using the GPRD. British journal of cancer. 2011; 104:193–7. [PubMed: 21081933]
46. McEvoy J, Flores-Otero J, Zhang J, Nemeth K, Brennan R, Bradley C, et al. Coexpression of normally incompatible developmental pathways in retinoblastoma genesis. Cancer Cell. 2011; 20:260–75. [PubMed: 21840489]
47. Li L, Hanahan D. Hijacking the Neuronal NMDAR Signaling Circuit to Promote Tumor Growth and Invasion. Cell. 2013; 153:86–100. [PubMed: 23540692]
48. Lee MJ, Ye AS, Gardino AK, Heijink AM, Sorger PK, MacBeath G, et al. Sequential application of anticancer drugs enhances cell death by rewiring apoptotic signaling networks. Cell. 2012; 149:780–94. [PubMed: 22579283]

NIH-PA Author Manuscript

NIH-PA Author Manuscript

NIH-PA Author Manuscript

Significance

Our work demonstrates the power of bioinformatics-based drug approaches to rapidly repurpose FDA-approved drugs and identifies a novel class of molecules to treat patients with SCLC, a cancer for which no effective novel systemic treatments has been identified in several decades. In addition, our experiments highlight the importance of novel autocrine mechanisms promoting the growth of neuroendocrine tumor cells.

NIH-PA Author Manuscript

NIH-PA Author Manuscript

NIH-PA Author Manuscript

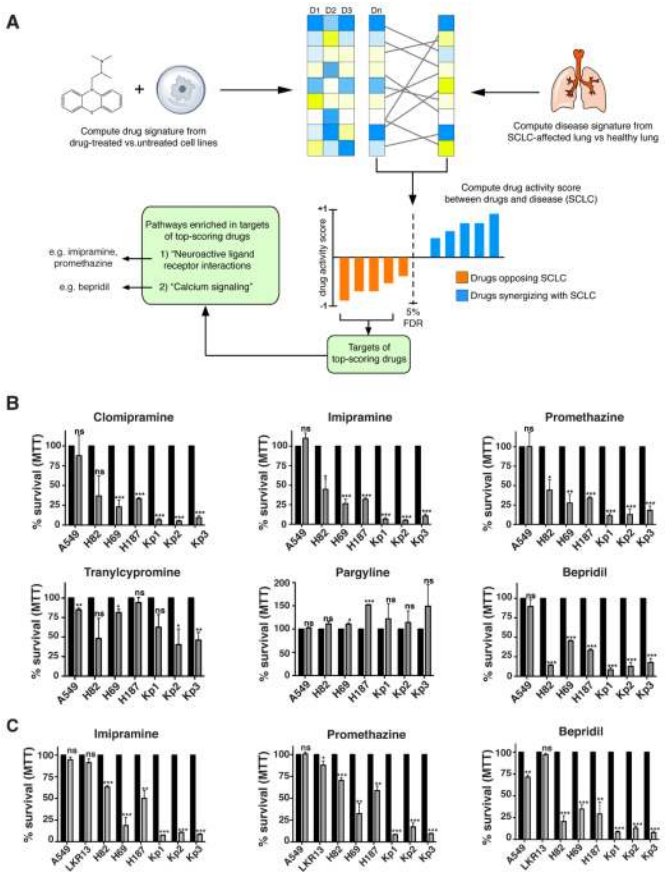

Figure 1. A bioinformatics-based drug repositioning approach identifies candidate drugs to inhibit SCLC

A, Schematic representation of the bioinformatics workflow for the repositioning approach used to identify potential candidate drugs for the treatment of SCLC. **B,** Representative MTT survival assays of cells cultured in 0.5% serum (n ≥3 independent experiments). A549 are NSCLC cells, H82, H69, and H187 are human SCLC cell lines, and Kp1, Kp2, and Kp3 are mouse SCLC cell lines. Cells were treated for 48 hours with 20μM clomipramine, 50μM imipramine, 30μM promethazine, 100μM tranylcypromine, 100μM pargyline, and 10μM bepridil. **C,** MTT survival assays of NSCLC (A549 and LKR13) and SCLC cells (H82, H69, H187, Kp1, Kp2, and Kp3) cultured in 2% serum (n>3 independent experiments) for 48 hours with 50μM imipramine, 30μM promethazine, and 10μM bepridil. Similar results were obtained in cells growing in dialyzed serum (data not shown). The black bars represent the vehicle-treated cells normalized to 100%. **P*<0.05, ***P*<0.01, and ****P*<0.001.

NIH-PA Author Manuscript
NIH-PA Author Manuscript
NIH-PA Author Manuscript

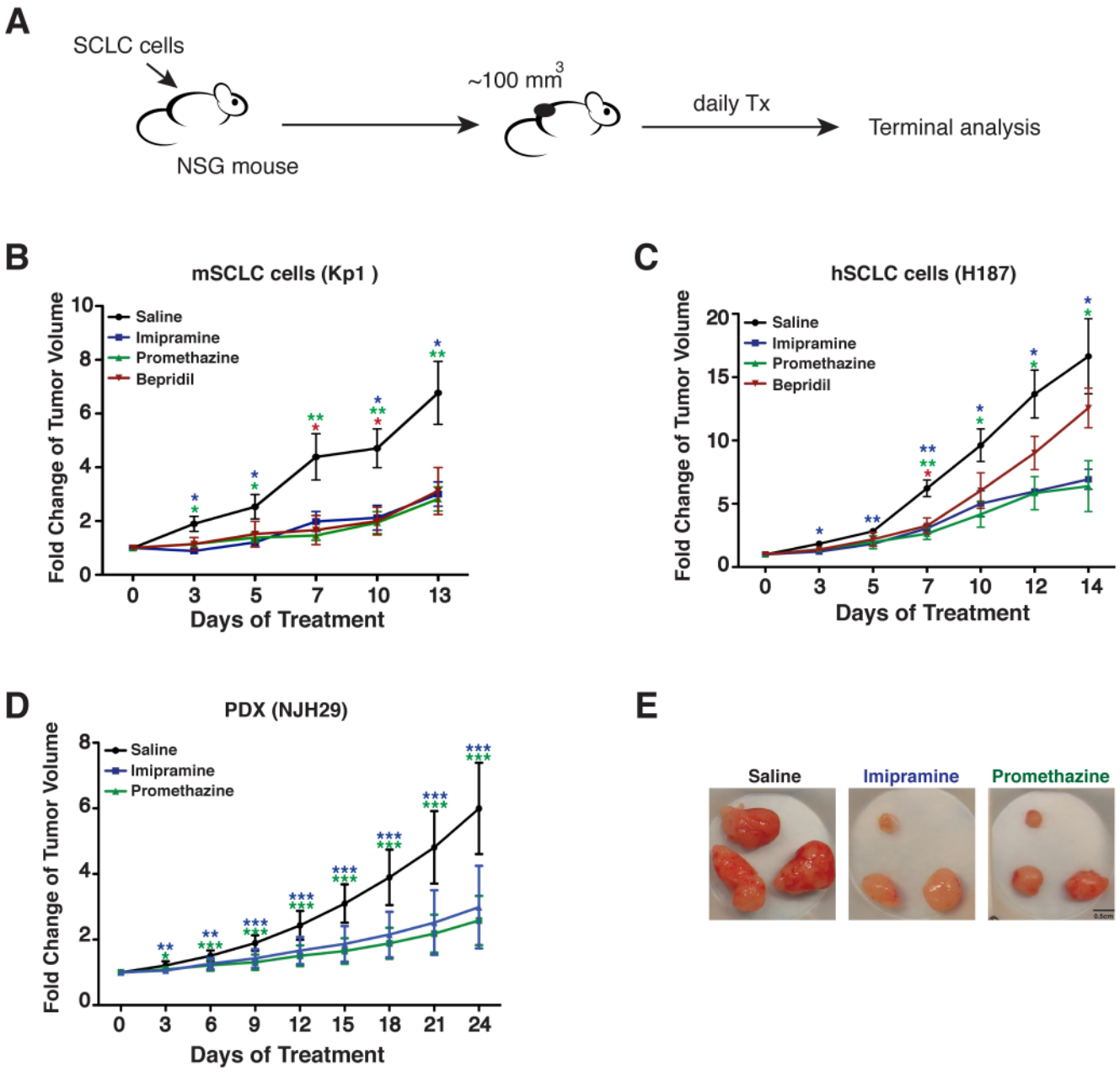

Figure 2. Inhibitory effects of imipramine, promethazine, and bepridil on SCLC allografts and xenografts

A, Strategy used for the treatment of mice growing SCLC allograft or xenograft tumors under their skin. NSG immunocompromised mice were subcutaneously implanted with one mouse SCLC cell line (Kp1) **(B)**, one human SCLC cell line (H187) **(C)**, and one primary patient-derived xenograft (PDX) human SCLC tumor (NJH29) **(D)**. Tumor volume was measured at the times indicated of daily IP injections with vehicle control (saline; n=8 in **(B)**, n=4 in **(C),** and n=12 in **(D)**), imipramine (25mg/kg; n=5 in **(B)**, n=4 in **(C)**, and n=12 in **(D)**), promethazine (25mg/kg; n=7 in **(B)**, n=4 in **(C),** and n=9 in **(D)**), and bepridil (10mg/kg; n=7 in **(B)** and n=3 in **(C)**) (3 independent experiments in **(B),** 1 experiment in **(C),** and 2 independent experiments in **(D)**). Values are shown as mean ± s.e.m. The unpaired t-test was used to calculate the p-values of imipramine- and promethazine- treated

NIH-PA Author Manuscript

NIH-PA Author Manuscript

NIH-PA Author Manuscript

tumors *versus* saline-treated tumors at different days of treatment. **P*<0.05, ***P*<0.01, and ****P*<0.001. Values that are not significant are not indicated**. E,** Representative images of the primary human SCLC xenografts (NJH29 cells) collected 24 days after daily treatment with saline, imipramine, and promethazine.

NIH-PA Author Manuscript

NIH-PA Author Manuscript

NIH-PA Author Manuscript

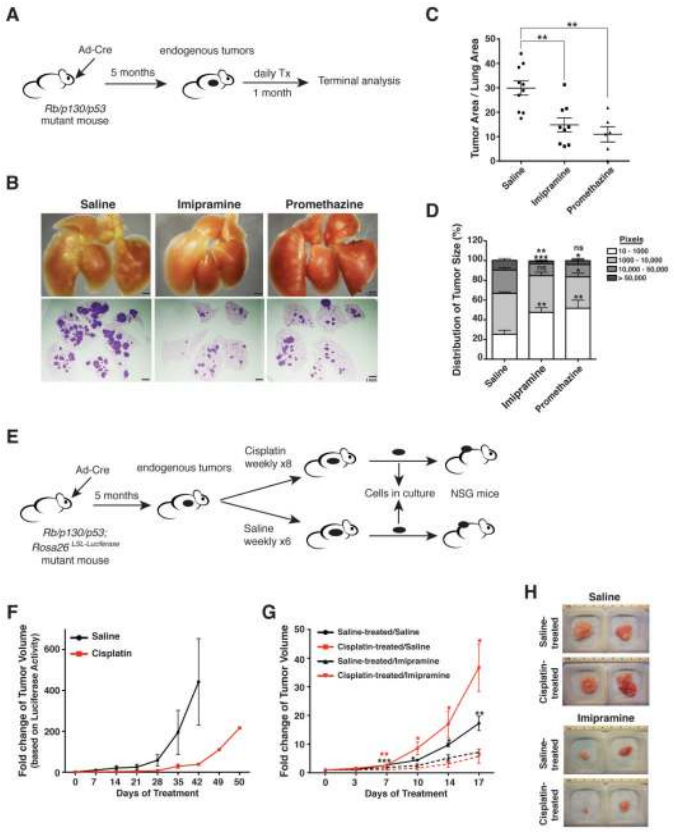

Figure 3. Imipramine and promethazine inhibit the growth of SCLC tumors in a pre-clinical mouse model

A, Strategy used for the treatment of *Rb/p53/p130* mutant mice developing endogenous SCLC tumors. **B**, Representative photographs of whole lungs and corresponding hematoxylin and eosin (H&E) stained sections from mutant mice 6 months after Ad-Cre infection, one month after the beginning of treatment with saline, imipramine (25mg/kg), or promethazine (25mg/kg). **C,** Quantification of the tumor surface area (pixel area units quantified by ImageJ) of mutant mice treated with saline (n=10), imipramine (n=9), and promethazine (n=6) (from 5 independent experiments). The unpaired t-test was used to calculate the p-values of imipramine-treated (*P*=0.0017) and promethazine-treated (*P*=0.0008) mice compared to control TKO mice. **D**, Bar graph showing the percentage size distribution of the tumors from mutant mice injected with saline (n=10), imipramine (n=9), and promethazine (n=5). Values are shown as mean ± s.e.m. **P*<0.05, ***P*<0.01, ****P*<0.001, ns, not significant. **E,** Strategy used for the treatment of *Rb/p53/p130;Rosa26*$^{lox\text{-}Stop\text{-}lox\text{-}Luciferase}$ mice developing endogenous SCLC tumors and treated with saline and cisplatin weekly to generate chemonaïve and chemoresistant tumors. Deletion of the *lox-Stop-lox* cassette by Cre allows expression of the reporter and measurement of tumor volume. **F,** Fold change of the tumor volume measured by luciferase activity in saline- and cisplatin-treated mice. **G,** NSG mice were subcutaneously implanted with the saline-treated and cisplatin-treated mouse SCLC cells shown in (**F)** and the fold change of the tumor volume was measured at the times indicated of daily IP injections with vehicle control (Saline n=4) and imipramine (25mg/kg; n=4). Values are shown as mean ± s.e.m. The unpaired t-test was used to calculate the p-values of imipramine-treated *versus* Saline-treated chemonaïve and chemoresistant tumors at different days of treatment. **P*<0.05, ***P*<0.01, and ****P*<0.001. Values that are not significant are not indicated. **H,**

Representative images of cisplatin- and saline-treated SCLC allografts collected 17 days after daily treatment.

NIH-PA Author Manuscript
NIH-PA Author Manuscript
NIH-PA Author Manuscript

NIH-PA Author Manuscript

NIH-PA Author Manuscript

NIH-PA Author Manuscript

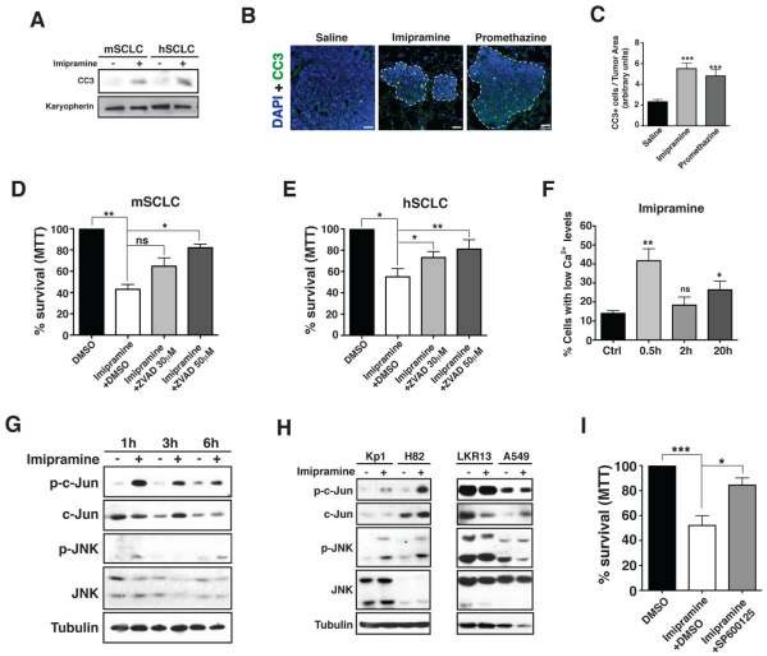

Figure 4. Imipramine and promethazine induce the apoptotic cell death of SCLC cells through activation of Caspase 3

A, Representative immunoblotting of cleaved Caspase 3 (CC3) in mSCLC (Kp1) and hSCLC (H82) cells treated with 50μM imipramine for 12 hours. Karyopherin was used as a loading control. **B,** Representative immunostaining of CC3 in tumor sections (white dashed lines) from *Rb/p53/p130* mutant mice treated daily with saline, imipramine, and promethazine for 30 consecutive days. **C,** Quantification of the percentage of CC3-positive cells per tumor area of saline- (n=142 tumors from 10 mice), imipramine- (n=153 tumors from 9 mice; $P<0.0001$), and promethazine- (n=103 from 6 mice; $P<0.0001$) treated tumors. **D–E,** Effects of the combined treatment of imipramine (50μM) and the pan-Caspase inhibitor Z-VAD-FMK on the survival of mSCLC **(D)** and hSCLC **(E)** after 24 hours of treatment, as measured by the MTT viability assay. Values from three independent experiments are shown as mean ± s.e.m. The paired t-test was used to calculate the p-values of imipramine-treated cells *versus* control DMSO-treated cells and of imipramine-treated cells *versus* Z-VAD-FMK- treated cells combined with imipramine. The black bars represent the vehicle-treated cells normalized to 100%. *$P<0.05$, **$P<0.01$, ***$P<0.001$, ns, not significant. **F,** Quantification of the percentage of mSCLC cells (Kp1 and Kp3) with low Ca^{2+} levels by FACS analysis of control untreated cells (Ctrl) and imipramine-treated cells at the times indicated. Values from three independent experiments for each cell line are shown as mean ± s.e.m. The unpaired t-test was used to calculate the p-values of imipramine-treated cells versus the untreated control cells at the times indicated. *$P<0.05$, **$P<0.01$, ***$P<0.001$, ns, not significant. **G,** Representative immunoblotting of p-c-Jun, total c-Jun, p-JNK, and total JNK in mSCLC cells (Kp1) treated with 50μM imipramine for the indicated times. Tubulin was used as a loading control. **H,** Representative immunoblotting of p-c-Jun, total c-Jun, p-JNK, and total JNK in mSCLC cells (Kp1 and H82) and NSCLC cells (LKR13 and A549) treated with 50μM imipramine for 1 hour. Tubulin was used as a loading control. **I,** Effects of the combined treatment of 50μM imipramine and 500nM of the JNK inhibitor SP600125 on mSCLC cells (Kp1) after 24 hours of treatment, as measured by the MTT viability assay. Values from three independent experiments are shown as mean ± s.e.m. The unpaired t-test was used to calculate the p-values of imipramine-treated cells *versus* control DMSO-treated cells and of imipramine-

treated cells *versus* SP600125-treated cells combined with imipramine. *P<0.05 and ***P<0.001.

NIH-PA Author Manuscript
NIH-PA Author Manuscript
NIH-PA Author Manuscript

NIH-PA Author Manuscript

NIH-PA Author Manuscript

NIH-PA Author Manuscript

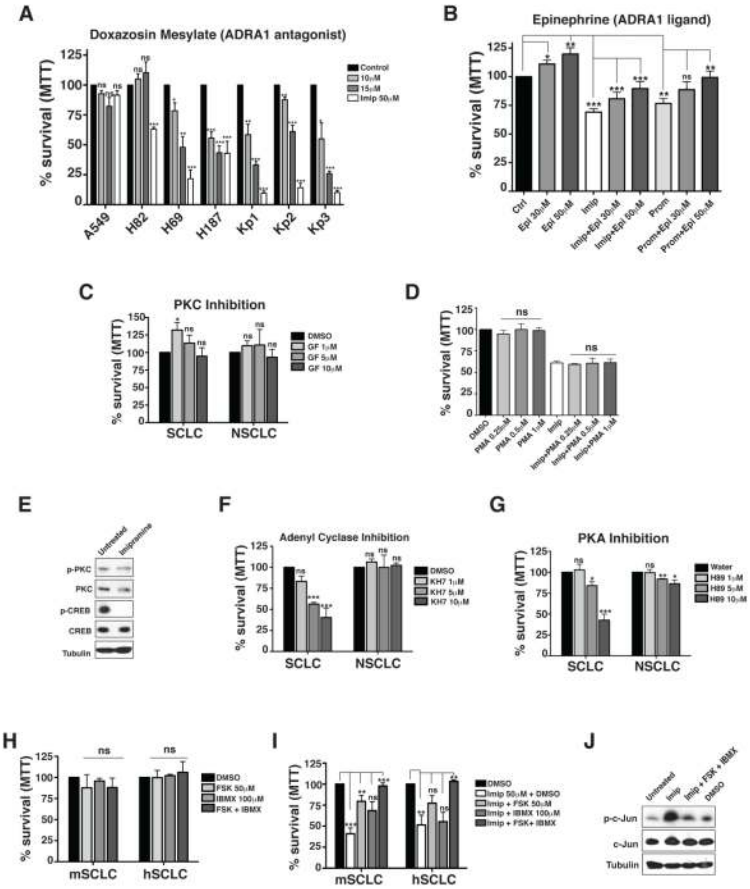

Figure 5. The candidate drugs inhibit the expansion of SCLC cells *via* several GPCRs

A–B, MTT viability assays of cells cultured at 2% serum (n ≥3 independent experiments) and treated with the ADRA1 antagonist doxazosin mesylate in comparison to treatment with imipramine (Imip) for 48 hours **(A)** and with increasing doses of epinephrine (Epi) in the absence or presence of 50μM imipramine (Imip) or 30μM promethazine (Prom) **(B)**. The paired t-test was used to calculate the p-values of epinephrine-, imipramine- and promethazine- treated cells *versus* control cells and of imipramine- and promethazine-treated cells *versus* epinephrine- treated cells combined with imipramine or promethazine. **P*<0.05, ***P*<0.01, ns, not significant. **C,** MTT viability assay for mSCLC (Kp1) and mNSCLC (LKR13) cells following 48 hours of treatment with increasing doses of the PKC inhibitor GF109203X. Values from three independent experiments are shown as mean ± s.e.m. The unpaired t-test was used to calculate the p-values of the drug-treated cells *versus* control cells. **P*<0.05, ns, not significant. **D,** MTT viability assay for mSCLC (Kp1) cells following 24 hours of treatment with 50μM imipramine alone and with increasing doses of PMA in the absence or presence of 50μM imipramine. The unpaired t-test was used to calculate the p-values of DMSO-treated cells versus PMA-treated cells and of imipramine-treated cells *versus* PMA-treated cells combined with imipramine. ns, not significant. **E,** Representative immunoblotting of p-PKC, total PKC, p-CREB, and total CREB in mSCLC cells (Kp1) untreated and treated with 50μM imipramine for 30 minutes. Tubulin was used as a loading control. **F–G,** MTT viability assay for mSCLC (Kp1) and mNSCLC (LKR13) cells following 48 hours of treatment with increasing doses of the adenyl cyclase inhibitor KH7 **(F)** and the PKA inhibitor H89 dihydrochloride **(G).** Values from three independent experiments are shown as mean ± s.e.m. The unpaired t-test was used to calculate the p-

NIH-PA Author Manuscript

NIH-PA Author Manuscript

NIH-PA Author Manuscript

values of the drug-treated cells *versus* control cells. **P*<0.05, ***P*<0.01, ****P*<0.001, ns, not significant. **H,** MTT viability assay for mSCLC (Kp1) and hSCLC (H187) cells following 24 hours of treatment with 50μM forskolin (FSK), 100μM IBMX, or both drugs combined. The unpaired t-test was used to calculate the p-values of the drug-treated cells *versus* control DMSO-treated cells. ns, not significant**. I,** Effects of the combined treatment of 50μM imipramine and 50μM FSK alone, 100μM IBMX alone, or FSK and IBMX together, as measured by the MTT viability assay. Values from at least three independent experiments are shown as mean ± s.e.m. The unpaired t-test was used to calculate the p-values of imipramine-treated cells *versus* control DMSO-treated cells and of imipramine-treated cells *versus* FSK-, IBMX-, and FSK+IBMX-treated cells combined with imipramine. **J,** Representative immunoblotting of p-c-Jun and total c-Jun in mSCLC cells (Kp1) untreated, treated with 50μM imipramine for 30 minutes in the absence or presence of 50μM forskolin (FSK) and 100μM IBMX, and treated with DMSO. Tubulin was used as a loading control. The black bars in all the MTT assays represent the vehicle-treated cells normalized to 100%.

NIH-PA Author Manuscript

NIH-PA Author Manuscript

NIH-PA Author Manuscript

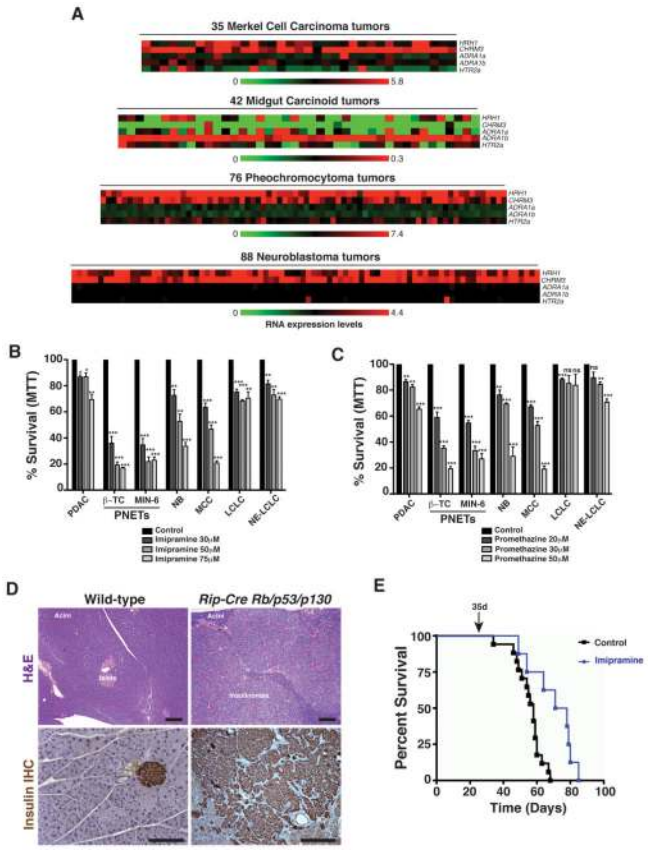

Figure 6. Tricyclic antidepressants inhibit the growth of several other types of neuroendocrine tumors

A, Heat maps showing the normalized RNA expression levels of the Histamine 1 Receptor (H1R), the Muscarinic Acetylcholine receptor isoform 3 (CHRM3), the Alpha1a and Alpha1b Adrenergic Receptors (ADRA1a and ADRA1b), and the Serotonin Receptor 2A (HTR2) in 35 human primary Merkel Cell Carcinoma tumors, 42 Midgut carcinoid tumors, 76 Pheochromocytoma tumors, and 88 Neuroblastoma tumors. **B–C,** MTT viability assays of human Pancreatic Adenocarcinoma (PDAC), mouse Pancreatic Neuroendocrine tumors (PNET), human Neuroblastoma (NB), human Merkel Cell Carcinoma (MCC), human large cell adenocarcinoma (LCLC) and neuroendocrine large cell carcinoma (NE-LCLC) cultured in low serum and treated with increasing doses of imipramine **(B)** and promethazine **(C)** for 48 hours. Values from three independent experiments are shown as mean ± s.e.m. **P*<0.05, ***P*<0.01, ****P*<0.001, ns, not significant. **D,** Representative H&E images (top) and insulin IHC (bottom) of sections from the pancreas of wild-type and *Rip-Cre Rb/p53/p130* (RIPCre-TKO) mutant mice. Scale bar is 50μm. **E,** Survival curve generated from the *Rip-Cre Rb/p53/p130* mice treated daily with IP injections of saline and imipramine starting at day 35 after birth; median survival is 58 days for saline- and 74.5 days for imipramine-treated mutant mice; p=0.024 by the Mantel-Cox test).

NIH-PA Author Manuscript

NIH-PA Author Manuscript

NIH-PA Author Manuscript

Table 1

Pathways significantly enriched among top-scoring SCLC repositioning hits.

Pathway name (KEGG ID)	Fold- enrichment	P-value	Gene targets
Neuroactive ligand- receptor interaction (hsa04080)	6.75	1.66×10^{-8}	*GABRA1, THRA, THRB, DRD2, GRIN3A, ADRA1, H1R, CHRM5, CHRM4, HTR1A, CHRM3, CHRM2, CHRM1, F2, ADRA1B, ADRA2A, ADRA1A, HTR2A*
Calcium signaling pathway (hsa04020)	5.99	3.13×10^{-4}	*CHRM5, HRH1, CHRM3, TNNC1, CHRM2, CHRM1, ADRA1B, ADRA1A, CACNA1A, CALM1, HTR2A*
Complement and coagulation cascades (hsa04610)	8.3	1.52×10^{-2}	*F10, F2, F9, F7, PROS1, PROC*

The unique set of canonical targets associated with the top-scoring SCLC repositioning hits was evaluated for biological enrichment in KEGG pathways using DAVID. The enrichment statistic p-values were adjusted for multiple testing using the Benjamini-Hochberg method, and pathways with and adjusted p-value < 0.05 are reported as being enriched for targets of top-scoring SCLC repositioning hits.